

Supplementary Informations

Defect Properties and Solution Energies of Dopants in NASICON-Type $\text{LiGe}_2(\text{PO}_4)_3$ Solid Electrolyte: A First-Principles Study

Anurup Das^{1,2}, Madhumita Goswami^{1,2} and P.S. Ghosh^{1,2,*}

¹Glass & Advanced Materials Division, Bhabha Atomic Research Centre, Mumbai 400085, India

²Homi Bhabha National Institute, Anushaktinagar, Mumbai 400094, India

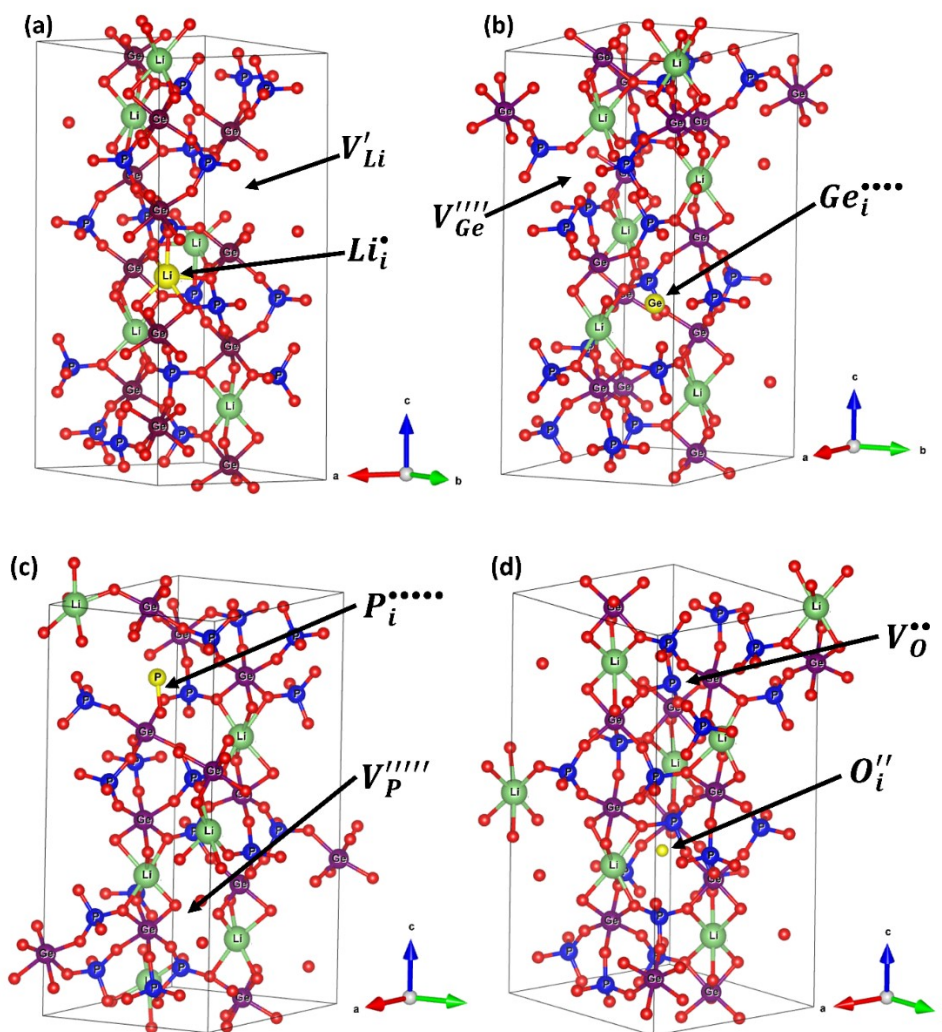


Fig. S11: Optimized unit cell of LGP containing different kinds of Frenkel defects

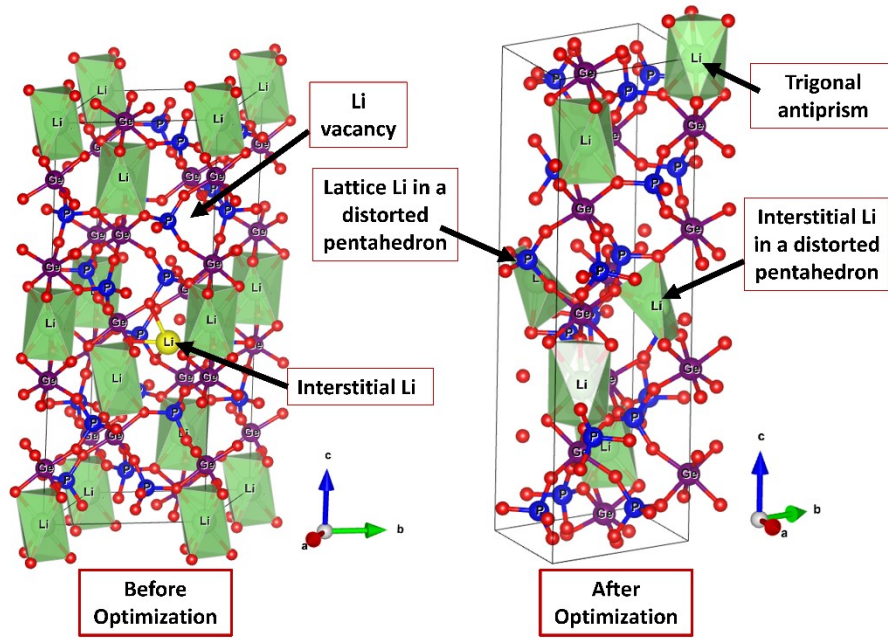


Fig. S12: Close observation on the structure with Li Frenkel defect

Table S11: Defects formation energies (eV/defect) reported previously

Li–TM antisite defects (at 1000 K)		Li ₁₂ TM ₁₂ O ₂₄	[1]
Li–Ni antisite defect concentration	12.9%	DFT calculations	
Li–Co antisite defect concentration	0.002%		
Li Frenkel pairs	~2 eV	Anti-perovskite	[2]
LiCl Schottky pair	1.41 eV	Li ₃ OCl	
Li ₂ O Schottky pair	1.60 eV	DFT calculations	
Li interstitial with a substitutional O on the Cl site	1.67 eV		
Li Frenkel	0.76	NASICON-type	[3]
Li ₂ O Schottky	3.59	LiTi ₂ (PO ₄) ₃	
		Classical MD	
Li Frenkel	0.75	NASICON-type	[4]
Ge/P antisite (isolated)	2.01	LiGe ₂ (PO ₄) ₃	
Ge/P antisite (cluster)	1.26	Classical MD	
Li ₂ O Schottky	3.10		
Li Frenkel	< 1 eV	Garnet-type	[5]
Li/La antisite (cluster)		Li ₇ La ₃ Zr ₂ O ₁₂	
Li ₂ O Schottky		DFT	
Li Frenkel	3.73	DFT/classical MD	[6]
Li ₂ O Schottky	9.20	LiNi _{1/3} Mn _{1/3} Co _{1/3} O ₂	
Li/M antisite	0.84 (Ni)		
Li Frenkel	1.76	LiMn ₂ O ₄	[7]
Li Frenkel	2.15	LiFePO ₄	[8]
Li ₂ O Schottky	6.33		

Li/M antisite	1.13		
Li Frenkel	1.97	LiMnPO ₄	[9]
Li ₂ O Schottky	7.36		
Li/M antisite	1.48		
Li Frenkel	1.21	Li ₂ FeP ₂ O ₇	[10]
Li/M antisite	0.22		

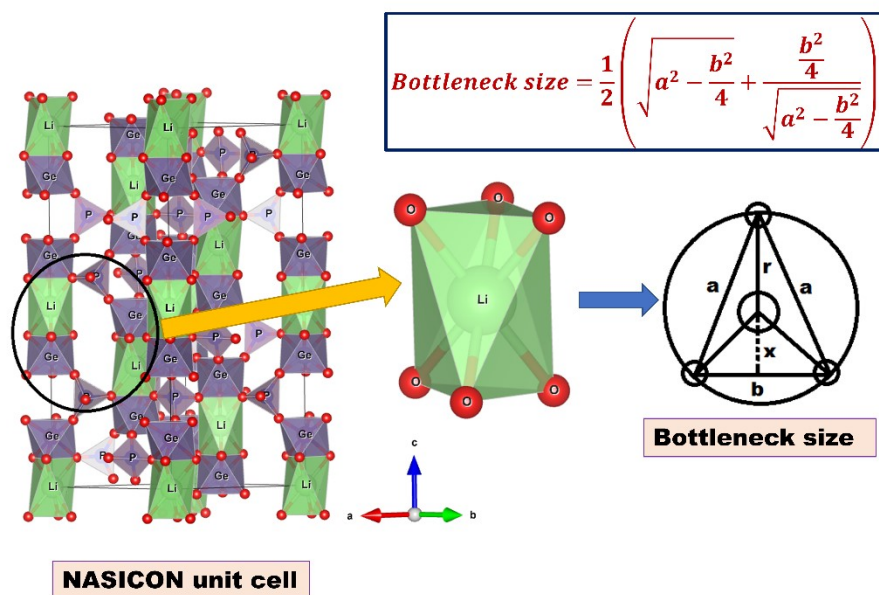


Fig. SI3: A schematic description of the bottleneck size calculation

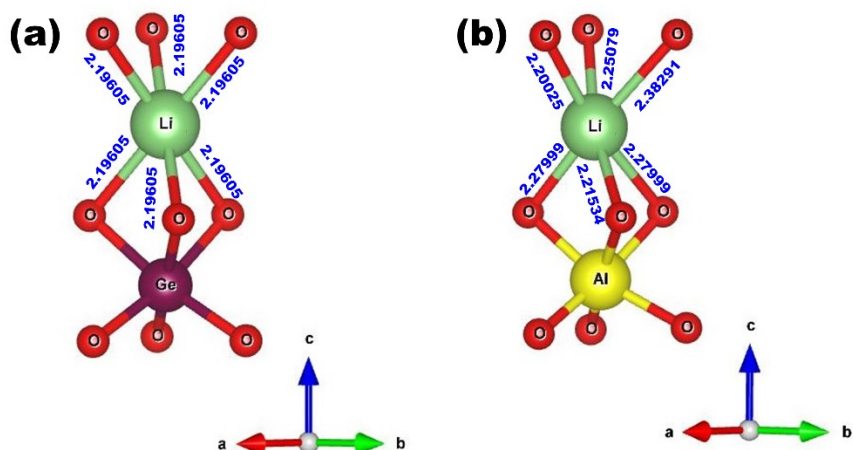
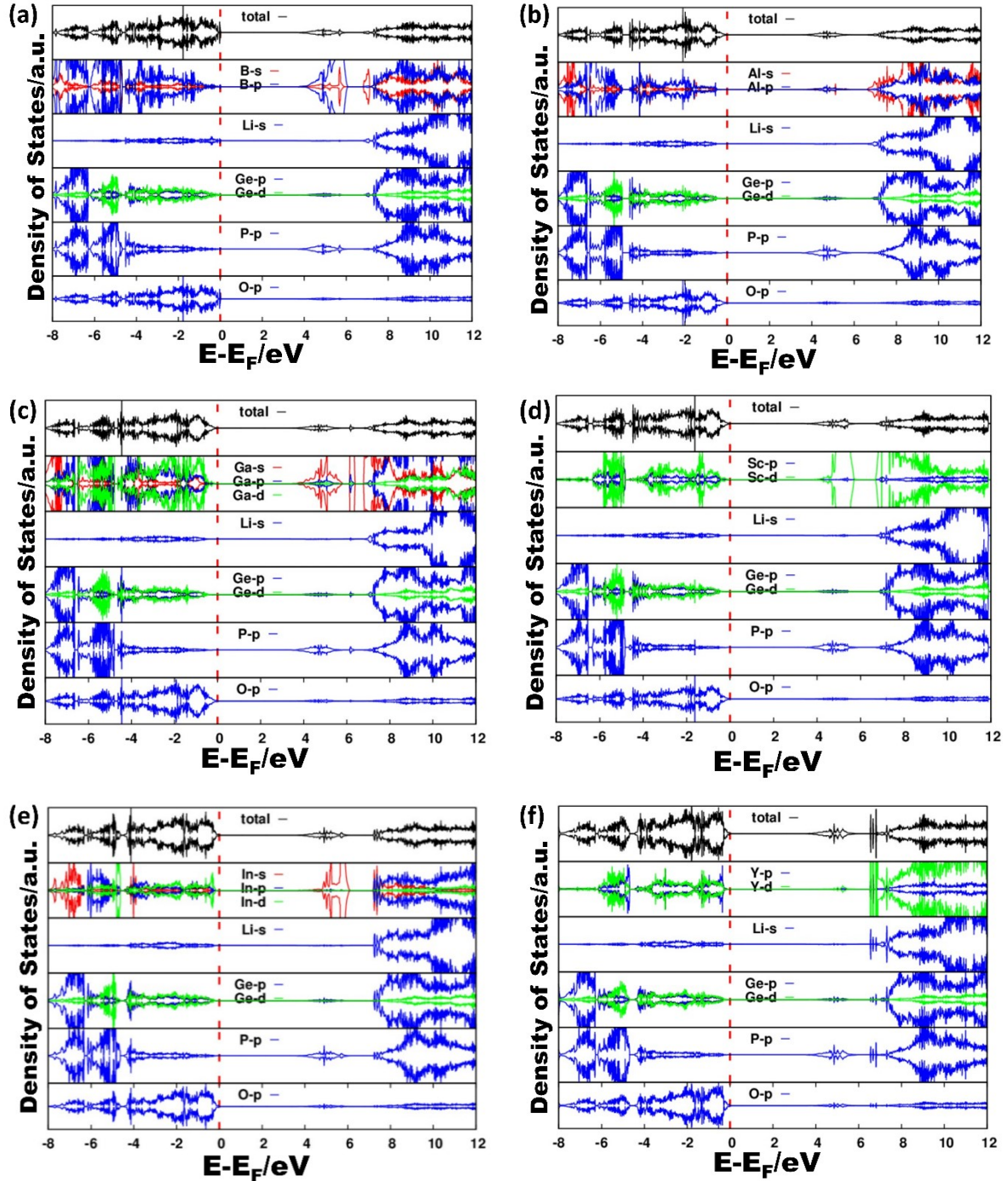


Fig. S14: LiO_6 and Ge/AlO_6 polyhedra taken from optimized unit cell of (a) before and (b) after substitution of Al^{3+} at Ge^{4+} position. The values of Li-O bond lengths are shown.



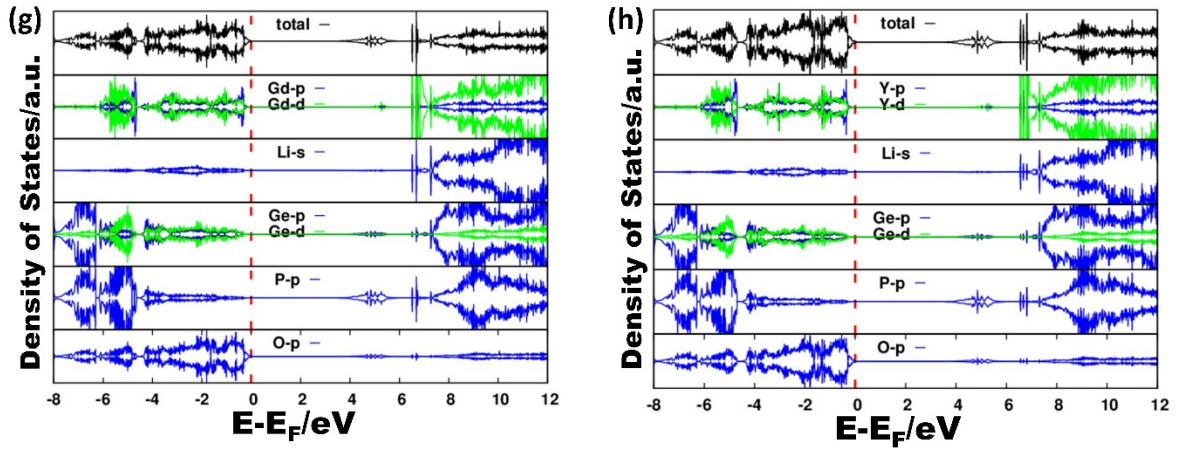


Fig. S15: Total and atom-projected partial density of states (DOS) for (a) B^{3+} , (b) Al^{3+} , (c) Ga^{3+} , (d) Sc^{3+} , (e) In^{3+} , (f) Y^{3+} , (g) Gd^{3+} and (h) La^{3+}

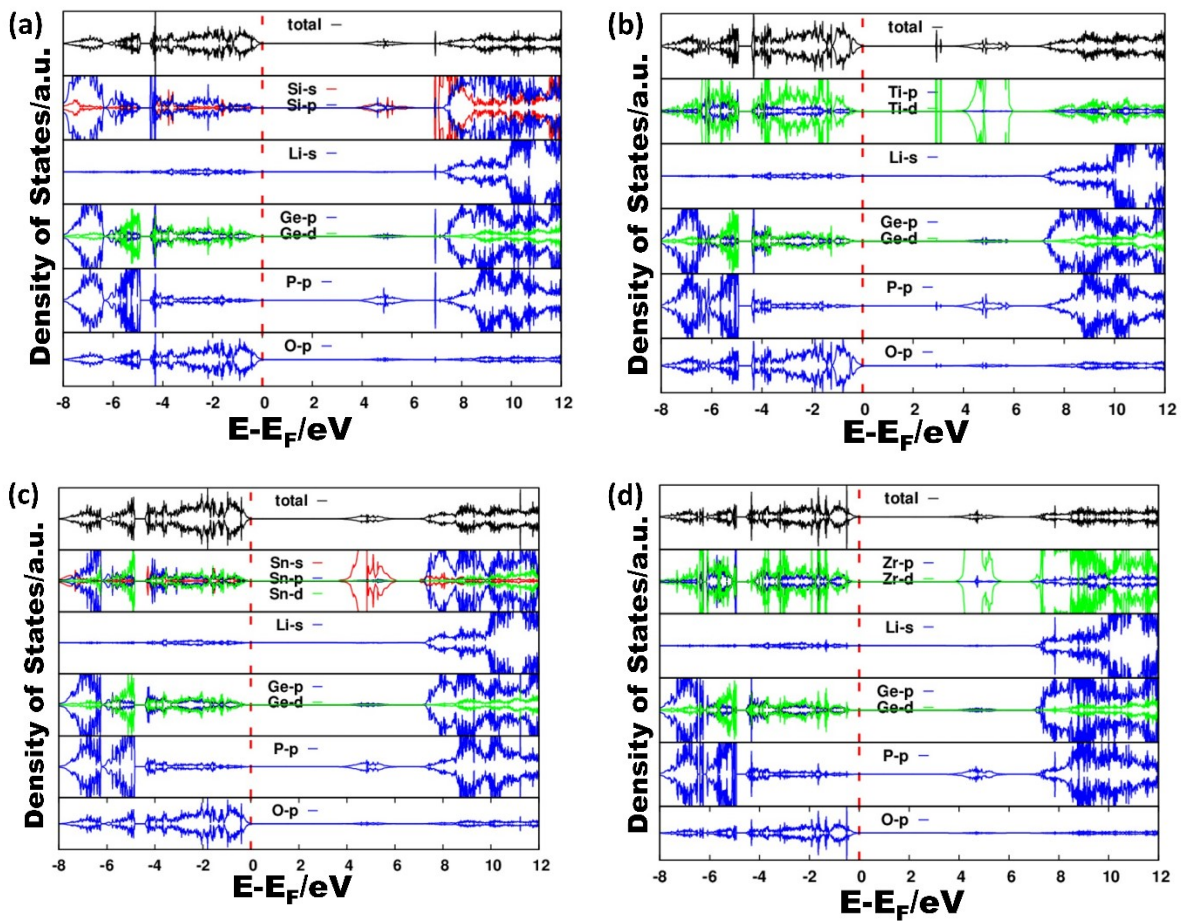


Fig. S16: Total and atom-projected partial density of states (DOS) for (a) Si^{4+} , (b) Ti^{4+} , (c) Sn^{4+} and (d) Zr^{4+}

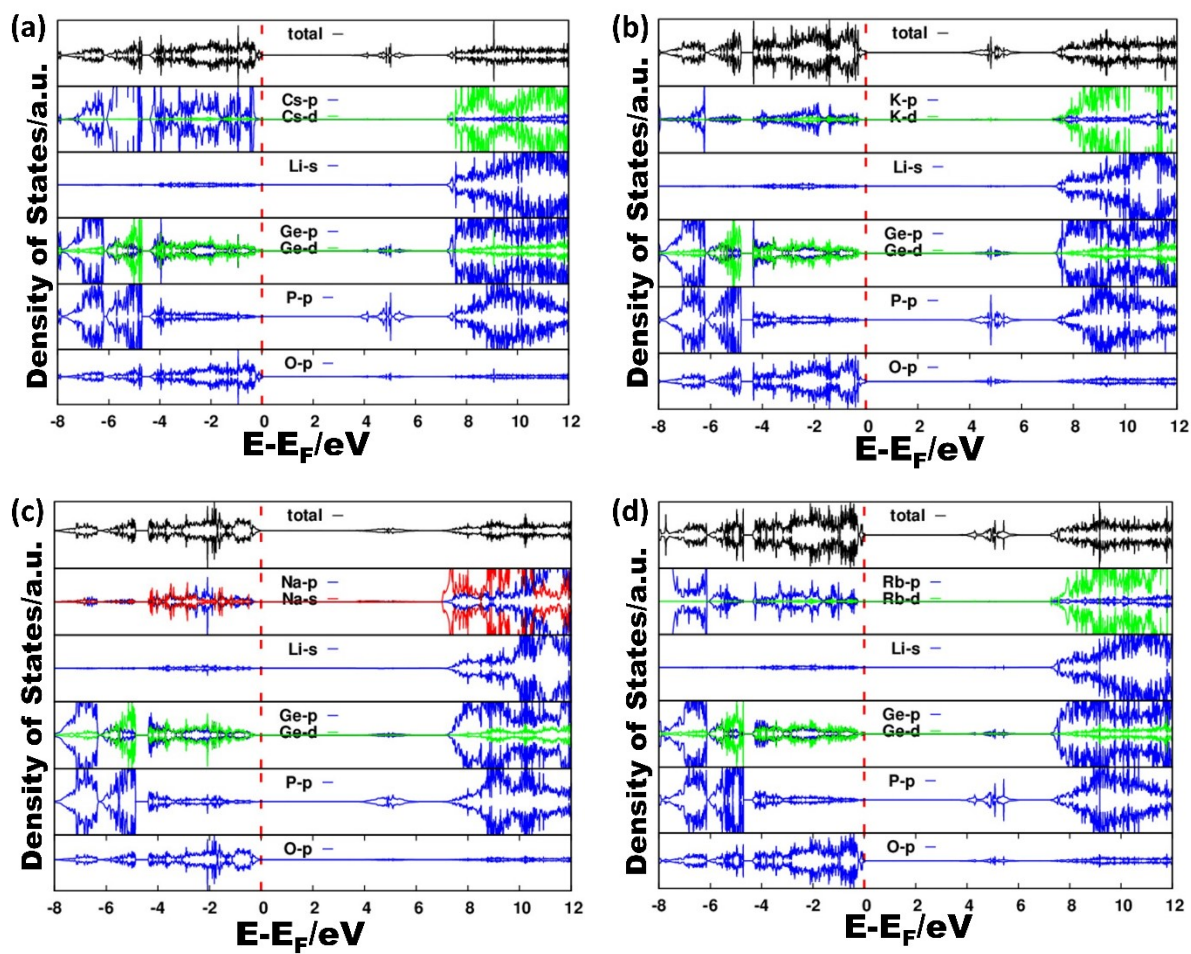
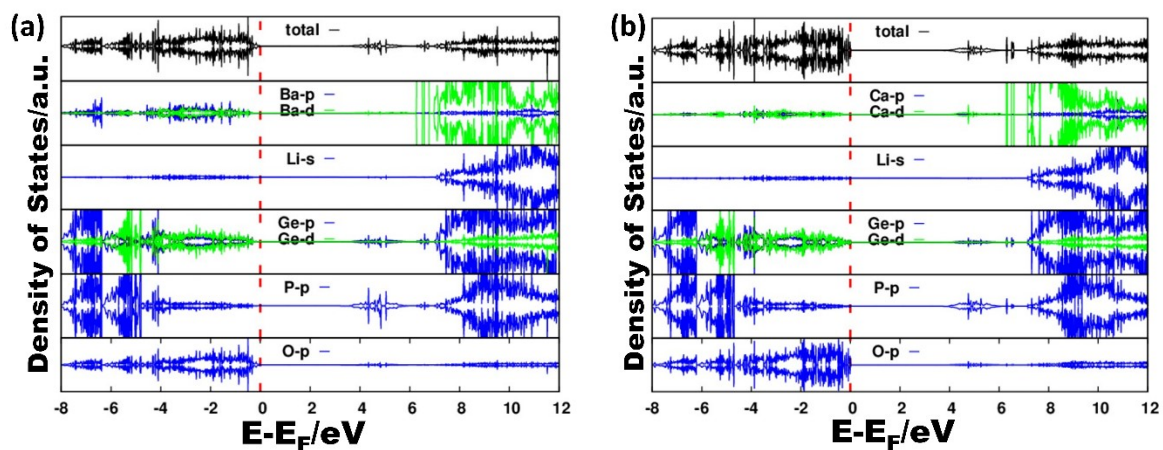


Fig. SI7: Total and atom-projected partial density of states (DOS) for (a) Cs⁺, (b) K⁺, (c) Na⁺ and (d) Rb⁺



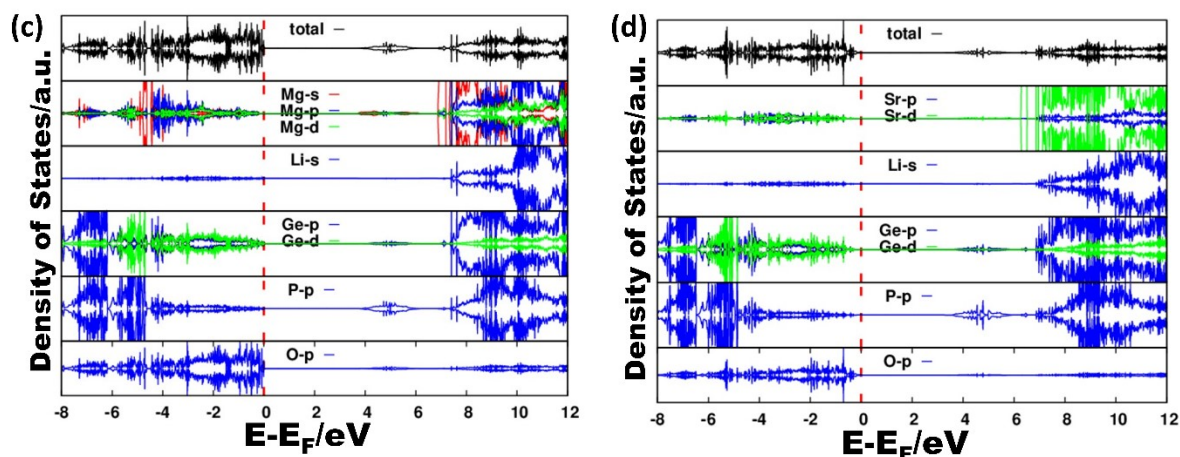


Fig. SI8: Total and atom-projected partial density of states (DOS) for (a) Ba^{2+} , (b) Ca^{2+} , (c) Mg^{2+} and (d) Sr^{2+}

References

- [1] Y. Kim, *Phys. Chem. Chem. Phys.*, 2019, **21**, 24139.
- [2] Z. Lu, C. Chen, Z.M. Baiyee, X. Chen, C. Niu, F. Ciucci, *Phys. Chem. Chem. Phys.*, 2015, **17**, 32547.
- [3] R. Sukumar, P. Iyngaran, N. Kuganathan, *Biointerface Res. Appl. Chem.*, 2021, **11**, 13268.
- [4] N. Kuganathan, K.A. Rex, P. Iyngaran, *Sustain. Chem.*, 2022, **3**, 404.
- [5] N. Kuganathan, M.J.D. Rushton, R.W. Grimes, J.A. Kilner, E.I. Gkanas, A. Chronos, *Sci. Rep.*, 2021, **11**, 451.
- [6] M.S. Islam, C.A. J. Fisher, *Chem. Soc. Rev.*, 2014, **43**, 185.
- [7] X. Li, J. Wang, S. Zhang, L. Sun, W. Zhang, F. Dang, H.J. Seifert, Y. Du, *ACS Omega*, 2021, **6**, 21255.
- [8] M.S. Islam, D.J. Driscoll, C.A.J. Fisher, P.R. Slater, *Chem. Mater.*, 2005, **17**, 5085.
- [9] C.A. J. Fisher, V.M.H. Prieto, M.S. Islam, *Chem. Mater.*, 2008, **20**, 5907.
- [10] J.M. Clark, S. Nishimura, A. Yamada, M.S. Islam, *Angew. Chem. Int. Ed.*, 2012, **51**, 1.